

Thesis Proposal

Solar Radiation Processes on the Antarctic Plateau: Interaction of Clouds, Snow, and Atmospheric Gases

Stephen R. Hudson

Department of Atmospheric Sciences
University of Washington

12 May 2005

General examination:
10:00 7 June 2005
Room 406 ATG

Abstract

A new set of measurements of the anisotropic reflectance factor of the snow surface on the high Antarctic Plateau will be used with the DISORT and ATRAD radiation models to learn about the combined effects of clouds, atmospheric gases and the snow surface on the solar radiation budget of the East Antarctic Plateau.

From the new data, a parameterization will be developed so that a relatively simple function will predict the anisotropic reflectance factor of the snow for a given set of viewing angles, solar zenith angle, and wavelength.

DISORT will be used, along with the new data, to model the bidirectional reflectance distribution function (BRDF) at the top of the atmosphere. This modeling will be compared with satellite observations and will help to explain those observations.

The effect of clouds on the BRDF at the top of the atmosphere will be investigated. It has been observed that clouds reduce the nadir reflectance over snow and increase the forward-scattering peak, despite the fact that cloud particles should be less forward-scattering than snow grains. A modeling investigation will try to explain the processes behind this effect.

Shortwave cloud radiative forcing at the surface and the top of the atmosphere over the Antarctic Plateau will be estimated using the ATRAD model and measurements made at Dome C and South Pole. These estimates will be compared with previous estimates made from both surface and satellite data.

Finally, the effects of carbon dioxide, ozone, and water vapor, atmospheric gases that absorb solar radiation, on the solar radiation budget will be investigated. Their effect on the planetary albedo over Antarctica will be modeled and the effects of the enhanced absorption by these gases due to the high surface albedo will be studied.

Table 1. A list of acronyms and symbols used in this proposal.

ATRAD	A spectral atmospheric radiation model
AVHRR	Advanced Very High Resolution Radiometer
BRDF	Bidirectional reflectance distribution function
CERES	Clouds and the Earth's Radiant Energy System
DISORT	A discrete ordinate radiative transfer model
ERBE	The Earth Radiation Budget Experiment
HDRF	Hemispherical-directional reflectance factor
L_i	Incident radiance
L_r	Reflected radiance
m_{im}	Imaginary index of refraction
MISR	Multi-angle Imaging Spectroradiometer
MODIS	Moderate Resolution Imaging Spectroradiometer
PAERI	Polar Atmospheric Emitted Radiance Interferometer
R	Anisotropic reflectance factor
SWCRF	Shortwave cloud radiative forcing
TOA	Top of the atmosphere
TOMS	Total Ozone Mapping Spectrometer
α	Albedo
θ_o	Solar zenith angle
θ_r	Viewing zenith angle
λ	Wavelength
ρ	Symbol for BRDF
ϕ	Relative azimuth angle (clockwise from ϕ_o to ϕ_r)
ϕ_o	Solar azimuth angle (clockwise from north)
ϕ_r	Viewing azimuth angle (clockwise from north)
ω_i	The element of solid angle from which light is incident

1. Introduction and Motivation

This project will explore the interactions of snow, clouds, and atmospheric gases with solar radiation over the East Antarctic Plateau. The two primary goals of the project are to better understand how snow, clouds and specific atmospheric gases combine to affect the intensity of reflected sunlight at the top of the atmosphere (TOA) and to determine the effect that clouds and specific atmospheric gases have on the solar energy budget, at both the surface and the TOA.

The East Antarctic Plateau covers an area of the globe roughly equal to that of the entire United States. For such a large area of land it has a remarkably homogeneous surface and climate. However, that climate, combined with its remote location, have largely kept people away, leaving many gaps in our basic understanding of the processes that control it.

Gaining a better understanding of this region's climate is crucial to understanding the regional and global effects of anthropogenic greenhouse gases. Obviously, like any significant area of the planet, changes in East Antarctica may affect the planet's energy balance; its high albedo means that there is a greater potential to increase the amount of solar energy absorbed in this region than in most parts of the planet. Climate changes in East Antarctica, the largest surface reservoir of fresh water on Earth, are also important for sea level; in a warming climate increased precipitation in this region may help to offset sea level rise caused by thermal expansion and melt of smaller bodies of ice. This study will help us better understand how possible future changes in cloud cover and atmospheric gases may affect both the local and global energy balance.

In recent decades satellite remote sensing has helped the climate community gain vast insight into the radiation components of global and regional energy budgets. The Earth Radiation Budget Experiment (ERBE) measured and calculated these radiation compo-

nents with unprecedented global coverage and its successor, Clouds and the Earth's Radiant Energy System (CERES), promises to continue this coverage with even better data.

However, remote sensing of the radiation components over Antarctica from satellites is still not fully reliable. Identifying clouds from satellites is difficult because of the low contrast between clouds and snow both in solar wavelengths, due to their similar spectral albedos, and in terrestrial wavelengths, due to the small temperature difference that often exists between the clouds and the surface (in fact, when a temperature difference does exist it very often confuses cloud detection algorithms because the clouds are often warmer than the surface). A second problem for remote sensors is one that they experience everywhere: their measure of radiance in one direction must be converted to a flux that integrates the radiance traveling in every direction in the upward hemisphere.

This study will provide estimates of the effects of clouds and gases on the solar radiation budget in East Antarctica that can be compared to those estimates from satellites. These estimates will be made from ground-based measurements and atmospheric radiation modeling, thus avoiding the problems remote sensors must handle. Additionally, the study will provide the remote sensing community with better information about the angular distribution of the reflected radiance over the plateau so that they may be able to convert their measurements to better estimates of flux.

The data used in this study will include *in situ* measurements of the angular distribution of reflected radiance from the snow surface, ground-based observations of cloud cover, and estimates of cloud optical depths from measurements of the spectrum of emitted radiation reaching the surface; the data were collected at the South Pole and at Dome C (75° S, 123° E), both on the East Antarctic Plateau. Satellite data from various platforms including the Advanced Very High Resolution Radiometer (AVHRR), the Moderate Resolution Imaging Spectroradiometer (MODIS), and the Multi-angle Imaging Spectro-

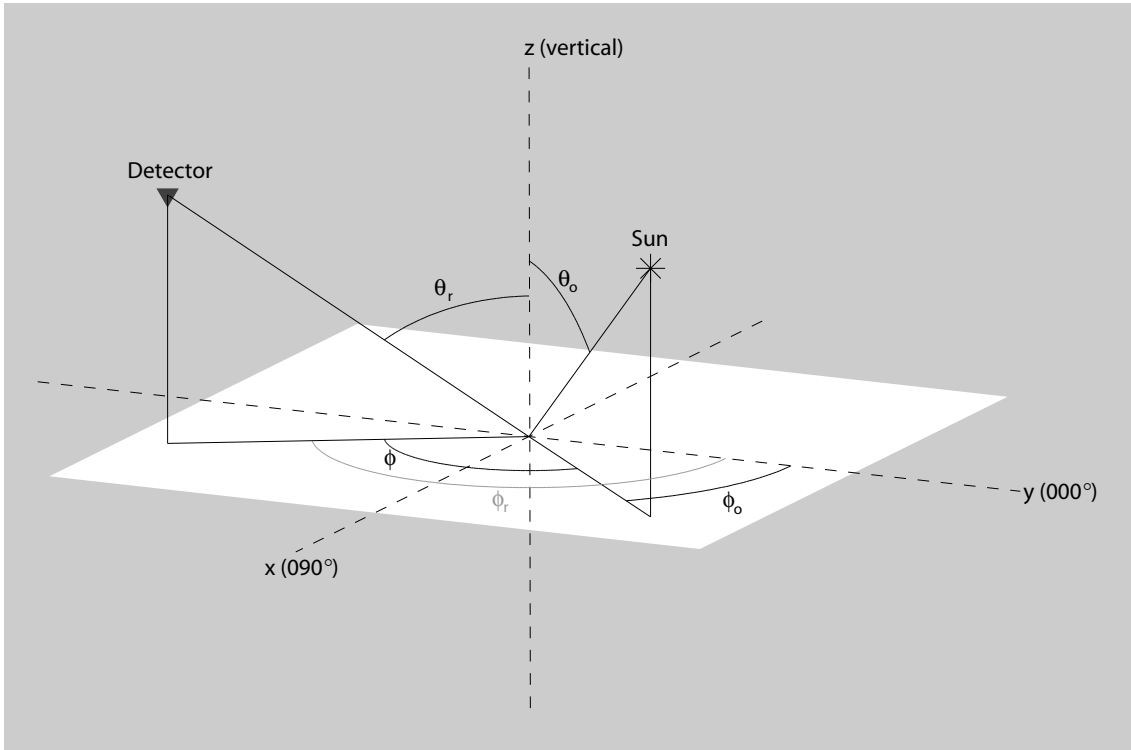


Figure 1. Definition of the solar zenith angle (θ_o), the viewing zenith angle (θ_r), the solar azimuth angle (ϕ_o), the viewing azimuth angle (ϕ_r), and the relative azimuth angle (ϕ).

radiometer (MISR) will also be used for comparison with modeled TOA radiances.

The next section of this proposal describes the data and models to be used. Sections 3 to 7 describe the five main proposed areas of research

2. Data and models

a. Terminology

This section describes the terminology that will be used throughout the rest of the proposal. Figure 1 illustrates the angles used to describe the angular distribution of reflected radiance. The necessary angles include the solar zenith (θ_o) and azimuth (ϕ_o , measured clockwise from north) angles and the viewing zenith (θ_r) and azimuth (ϕ_r) angles.

The two azimuth angles can be reduced to one relative azimuth angle (ϕ), the viewing azimuth measured clockwise from the solar azimuth, if there is no preferred orientation to

the surface roughness. This criterion is not always met on the Antarctic Plateau because long, erosional dunes with heights of tens of centimeters, known as sastrugi, typically form with their long axes aligned with the prevailing wind. However, Warren et al. (1998) showed that the effect of the sastrugi on the angular reflectance pattern was minimal for $\theta_r \lesssim 50^\circ$. Additionally, the data to be used in this study were collected near the top of one of the ice domes, where winds are lighter and less directionally constant than on other parts of the plateau, resulting in smaller and less well-aligned sastrugi. These two observations will allow the use of ϕ in this study.

There are numerous ways in which the angular distribution of reflected radiance may be described. Nicodemus et al. (1977) defined the bidirectional reflectance distribution function (BRDF) as the ratio of the radiance reflected into a particular direction to the incident flux, all of which is coming from a single direction:

$$\rho = \frac{L_r(\theta_o, \theta_r, \phi)}{L_i(\theta_o) \cos \theta_o d\omega_i}, \quad (1)$$

where L is radiance, and the subscripts r and i indicate whether the radiance is reflected or incident. This quantity is relevant to satellite measurements, where the incident light is all coming from the direction of the sun, in which case $L_i d\omega_i$ is the normal-incidence solar flux, and is not dependent on θ_o .

When measurements are made at the surface the incident flux comes from a combination of direct-beam illumination by the sun and diffuse (but not isotropic) illumination from the entire sky due to Rayleigh and other atmospheric scattering. Surface measurements can be used to describe the hemispherical-directional reflectance factor (HDRF), which Nicodemus et al. (1977) defined as the ratio of the radiance reflected into a particular direction to the incident flux from all directions in the upward hemisphere. At short wavelengths, surface-based measurements of HDRF differ significantly from the BRDF that would be measured if there were no diffuse light, but, because of the strong wave-

length dependence of Rayleigh scattering and the small aerosol concentration above the Antarctic Plateau, by about 800 nm the measured HDRF under clear skies is nearly identical to the BRDF because over 95% of the incident flux is in the direct beam (Grenfell et al. 1994). For this reason, and because the measurements made at the surface with a diffuse component are the relevant geophysical measurements, the distinction between BRDF and HDRF will be ignored.

It is often convenient to nondimensionalize and normalize the BRDF, a step which also eliminates the need to accurately measure the incident flux. Suttles et al. (1988) defined an anisotropic reflectance factor, R , as the ratio of the equivalent-Lambertian reflected flux (π times the reflected radiance) to the actual reflected flux:

$$R(\theta_o, \theta_r, \phi) = \frac{\pi L_r(\theta_o, \theta_r, \phi)}{\int_0^{2\pi} \int_0^{\pi/2} L_r(\theta_o, \theta_r, \phi) \cos \theta_r \sin \theta_r d\theta_r d\phi}. \quad (2)$$

This function is not only nondimensionalized, it is also normalized; i.e.,

$$\frac{1}{\pi} \int_0^{2\pi} \int_0^{\pi/2} R(\theta_o, \theta_r, \phi) \cos \theta_r \sin \theta_r d\theta_r d\phi = 1. \quad (3)$$

Recognizing that the albedo (the ratio of reflected to incident flux) is

$$\alpha(\theta_o) = \int_0^{2\pi} \int_0^{\pi/2} \rho(\theta_o, \theta_r, \phi) \cos(\theta_r) \sin(\theta_r) d\theta_r d\phi, \quad (4)$$

we can rewrite R in terms of α and ρ :

$$R(\theta_o, \theta_r, \phi) = \frac{\pi}{\alpha} \rho(\theta_o, \theta_r, \phi). \quad (5)$$

b. Data

This project will make use of a new set of observations of the anisotropic reflectance factor of the Antarctic snow surface. These data were collected during the austral summers of 2003/04 and 2004/05 at Dome C Station, located at 75° S 123° E, at an elevation

of 3250 m above sea level. They represent the most extensive set of observations of their kind made in Antarctica, covering a spectral range of 350 to 2500 nm at one-nanometer resolution and a range of solar zenith angles from 52° to 87° .

These measurements were made from atop a 32-meter tower positioned so that a 255° range of azimuths containing undisturbed snow could be viewed. A fiber optic with a 15° -diameter circular field of view was attached to a spectroradiometer to make the measurements. The open end of the fiber was mounted in a goniometer that allowed it to be accurately positioned at specific viewing zenith and azimuth angles.

Since measurements could be made from only a 255° range of azimuths, some assumptions must be made to determine R , a function normalized over the entire hemisphere. The missing angles are filled in using two separate methods, depending on which relative azimuths are missing. For observations which include both $\phi = 0^\circ$ and $\phi = 180^\circ$, symmetry across the principal plane (the plane normal to the surface that contains both the sun and the detector) is assumed, and the complete half pattern that is available is reflected across the principal plane. For example, at noon, observations cover relative azimuths from 150° clockwise through 30° ; those measurements with $180^\circ \leq \phi \leq 360^\circ$ are retained and are reflected to fill radiances from $180^\circ \geq \phi \geq 0^\circ$, so

$$L_r(\theta_o, \theta_r, \phi = 45^\circ) = L_r(\theta_o, \theta_r, \phi = 315^\circ).$$

In this case, if this assumption is true, we should expect the radiances measured at 195° , 210° , 330° , and 345° to equal those at 165° , 150° , 30° , and 15° , respectively. Qualitative checks of this sort during preliminary analyses support the assumption of symmetry across the principal plane. Observations that do not include both $\phi = 0^\circ$ and $\phi = 180^\circ$ are combined with another observation taken on the same or adjacent day when θ_o was the same but ϕ_o was different (within a 48-hour period, θ_o is approximately equal at times equally distant from noon). In these cases there are always some relative azimuths that

are included in both observations; these are used to find a scale factor that minimizes differences in radiances due to atmospheric changes between the two times.

These observations resulted in 98 complete patterns of the anisotropic reflectance factor of the snow surface at Dome C, providing good coverage of most solar zenith angles in the range 52° to 87° .

During the 2003/04 summer a Polar Atmospheric Emitted Radiance Interferometer (PAERI) was operated on the same tower from which the anisotropic reflectance factor was measured. The PAERI measured the emitted infrared radiance from the zenith approximately every 10 minutes. Similar data are also available from South Pole from the summer of 2000/01. From these data the infrared optical depths of summertime clouds can be determined, from which the visible optical depth can be estimated.

Visible and near-infrared radiances from polar orbiting satellites will be obtained. The data from MODIS and MISR are available as geolocated calibrated radiances from NASA, and the International Satellite Cloud Climatology Project's B2 data set provides AVHRR radiances sampled at 30-kilometre resolution; it is available from the National Climatic Data Center.

Data that may be useful for atmospheric modelling include profiles of temperature and humidity measured with radiosondes launched at Dome C twice-daily during summer 2003/04 and ozone concentration data from the Total Ozone Mapping Spectrometer (TOMS) on board NASA's Earth Probe satellite.

c. Models

Two radiation models will be used in this study. A discrete ordinate radiative transfer model (DISORT) developed by Stamnes et al. (1988) and a spectral atmospheric radiation model (ATRAD, Wiscombe et al. 1984) that includes molecular absorption.

The DISORT method solves, with arbitrary accuracy, the radiative transfer equation for a vertically-inhomogeneous, plane-parallel atmosphere. The model can calculate the monochromatic flux and radiance in any direction at each model layer. The atmosphere is described as consisting of numerous layers, each of which has uniform single scattering albedo and phase function within the layer, though these parameters may differ between layers. Each layer may have a different optical depth. The upper boundary condition can be specified as including a direct-beam source, a diffuse source, or both. The BRDF of the lower boundary is specified by the user.

In DISORT, the phase function is described with a series of $2N$ Legendre polynomials and the intensity as a Fourier series of order $2N$. Larger values of N produce a more accurate solution, allowing for an arbitrarily accurate solution.

The ATRAD model is a spectral model, with spectral resolution up to 20 cm^{-1} . It assumes a plane-parallel atmosphere with an arbitrary number of layers and calculates both flux and radiance across an arbitrary spectral range. ATRAD handles molecular absorption by using sums of exponentials to fit the LOWTRAN transmission functions (equivalent to the “k-distribution” method). Multiple scattering is treated with the adding-doubling method.

3. Analysis and Parameterization of the Dome C BRDF

The first step in this project is the analysis of the data collected at Dome C. With 98 complete BRDF observations at 2150 wavelengths, it is obviously necessary to automate this process somewhat. I have written software to read the raw radiances, average them over a specified wavelength interval, account for the variations in θ_o and ϕ_o during the time the observation was made, and produce full patterns of R . Some of these results are shown in Figures 2 through 4.

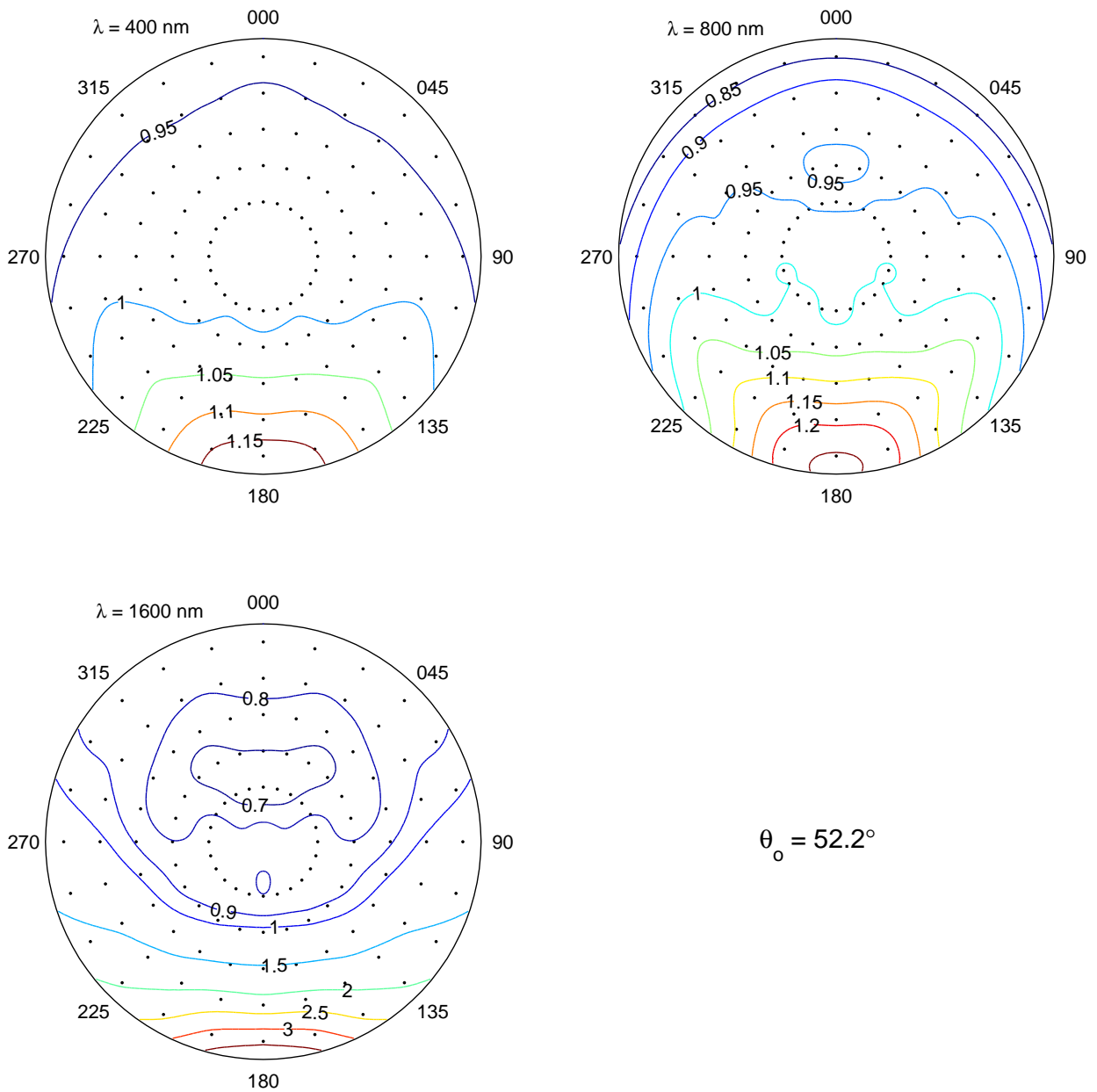


Figure 2. Polar contour plots of the anisotropic reflectance factor (R) measured on 5 January 2004 at 11:38 local standard time (LST), with a solar zenith angle of 52.2° . Results for three wavelengths are shown: 400 nm (upper left), 800 nm (upper right), and 1600 nm (bottom). The dots are located every 15° in ϕ at nadir angles of 22.5° , 37.5° , 52.5° , 67.5° , and 82.5° . Note that the contour interval sometimes changes at 1.0.

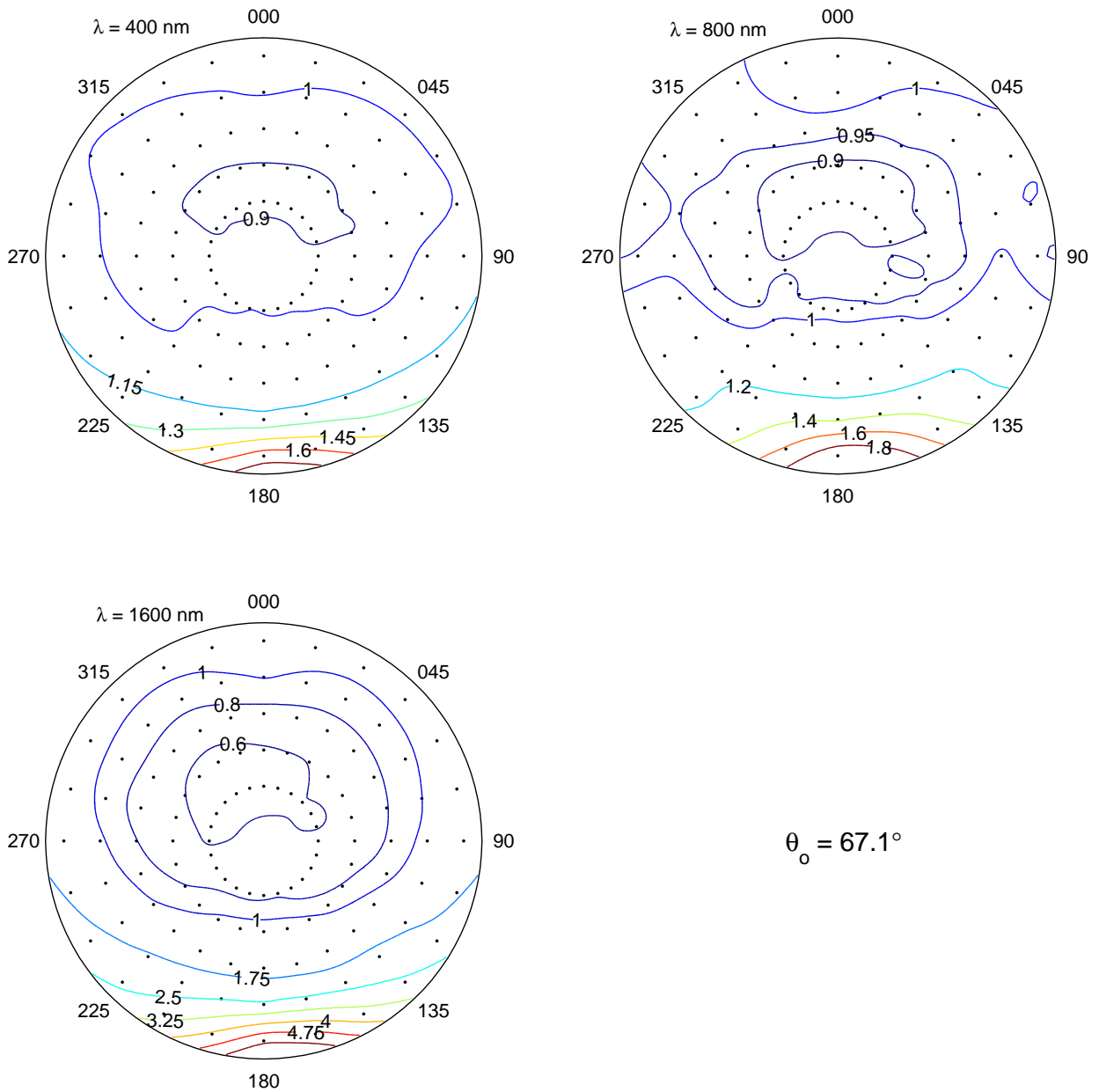


Figure 3. Polar contour plots of the anisotropic reflectance factor (R) measured on 10 January 2004 at 17:18 LST and 11 January 2004 at 06:09 LST, with a solar zenith angle of 67.1° . Results for three wavelengths are shown: 400 nm (upper left), 800 nm (upper right), and 1600 nm (bottom). The dots are located every 15° in ϕ at nadir angles of 22.5° , 37.5° , 52.5° , 67.5° , and 82.5° . Note that the contour interval sometimes changes at 1.0.

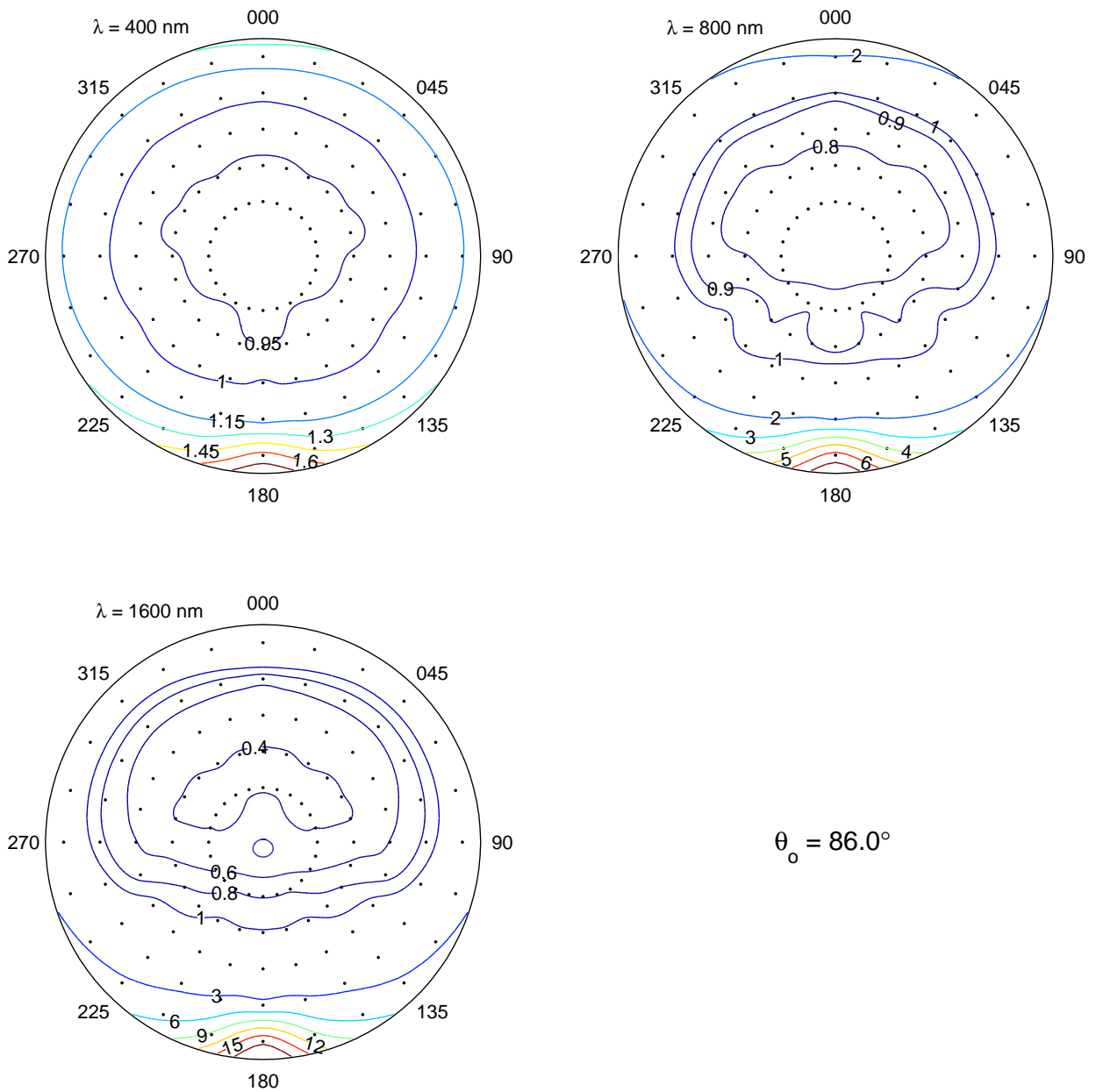


Figure 4. Polar contour plots of the anisotropic reflectance factor (R) measured on 27 January 2005 at 22:48 LST, with a solar zenith angle of 86.0° . Results for three wavelengths are shown: 400 nm (upper left), 800 nm (upper right), and 1600 nm (bottom). The dots are located every 15° in ϕ at nadir angles of $22.5^\circ, 37.5^\circ, 52.5^\circ, 67.5^\circ,$ and 82.5° . Note that the contour interval sometimes changes at 1.0.

In these three figures R is contoured for three different solar zenith angles (52° , 67° , and 86°) at three wavelengths (400, 800, and 1600 nm). The three wavelengths were chosen to illustrate two separate ways in which R is dependent on wavelength.

First, to illustrate the effect of absorption by ice, consider that the imaginary index of refraction (m_{im}) of ice at 400, 800, and 1600 nm is 2.82×10^{-9} , 1.34×10^{-7} , and 2.70×10^{-4} (Warren 1984; Kou et al. 1993). While m_{im} changes significantly across both wavelength intervals, the resulting change in albedo is significantly greater between 800 and 1600 nm [the albedo is about 0.98, 0.92, and 0.08 for the three wavelengths with a solar zenith angle of 60° and snow grain radius of 100 μm (Wiscombe and Warren 1980)] because the mean distance traveled by a photon in ice before it is absorbed ($\frac{\lambda}{4\pi m_{im}}$) is 11 m, 50 cm, and 500 μm at 400, 800, and 1600 nm; since a typical snow grain has a diameter on the order of 100 μm , this means photons with either of the two shorter wavelengths can expect to travel through thousands of snow grains before being absorbed, while at the longest wavelength they are likely to survive through only a few snow grains. This difference means that most of the relatively few 1600-nanometer photons that emerge from the snow have been scattered only a few times, which allows the strongly anisotropic single-scattering phase function of the snow grains to cause a more anisotropic BRDF than in the two shorter wavelengths.

A second dependence on wavelength results from the strong wavelength dependence of Rayleigh scattering. At 400 nm a significant portion of the downwelling flux at the surface, between 25% and 40% (Grenfell et al. 1994), is in the form of diffuse light from the entire sky, while at the two longer wavelengths almost all of the downwelling flux at the surface is in the direct solar beam. This large amount of diffuse flux at short wavelengths decreases the anisotropy of the BRDF.

The three figures also illustrate that R depends on the solar zenith angle. The larger the

solar zenith angle, the more anisotropic the BRDF; this effect is greater at wavelengths that were strongly anisotropic at smaller solar zenith angles. This dependence on solar zenith angle is largely due to the fact that, with a low sun, a photon can more easily escape the snow as a result of forward scattering events, which are the most likely scattering events. With a high sun, forward scattering events tend to send the photons deeper into the snow and their directions become more randomized before they escape. The effect is damped at short wavelengths because a low sun also results in more diffuse radiation where there is significant scattering.

The exact symmetry about the principal plane (in these plots, a vertical line connecting 000° and 180°) seen in Figures 2 and 4 is a result of the reflection method used to create these patterns. The relatively minor asymmetries seen in Figure 3 are probably mostly due to minor changes in the atmosphere between the two observation times and to instrument noise, but could also be due to slight anisotropy of the surface roughness.

In an effort both to more easily use these data in the rest of this project and to provide these data to the climate community in a more useful form, R will be parameterized as a function of solar zenith angle, viewing zenith angle, relative azimuth, wavelength, and imaginary index of refraction. I have already made some progress on this effort, and the preliminary results were promising, but more work is needed to either come up with one parameterization for all angles, or to produce separate parameterizations for high and low sun cases.

4. Satellite-observed BRDF

The observed anisotropic reflectance factors, measured under clear skies, will be used as the lower boundary layer in DISORT to predict the TOA BRDF. These modeled results will then be compared to TOA BRDF observed by satellites viewing the Dome C region.

This procedure will be carried out for various visible and near-infrared channels on different satellites for a variety of solar zenith angles. It will allow for a test of the model's ability to accurately determine the TOA radiances and will also provide for a test of the best configuration of the model.

While the Dome C observations are at a spectral resolution of 1 nm, the satellite measurements are made with wider channels; the visible and near-infrared channels on AVHRR include 0.58 to 0.68 μm , 0.725 to 1.1 μm , and 1.58 to 1.64 μm . The satellites' use of wider bands means that an appropriate spectrally-averaged value of R , with the average weighted by the channel response function, will have to be used as the lower boundary condition, and appropriate values of the single-scattering albedo and phase function for the spectral band must be determined for the atmospheric layers. Alternatively, the band could be broken up into smaller bands, each of which would be modeled individually, and then combined to determine the values for the entire band. The latter approach is more straight forward, and is likely to be more accurate.

Satellites do not measure the entire BRDF of any location. Each time they pass over an area they measure the radiance from only one or two angles, so it will be these individual angles that are compared. The high-latitude location of Dome C means that there are numerous overpasses by polar-orbiting satellites each day, providing for many possible comparisons.

Because satellites measure the radiance from a given location at only a limited number of viewing angles, users of satellite data must try to determine the entire BRDF from relatively few radiance values. In an effort to assist in this process, the Dome C data, along with the modeled TOA BRDFs will be used to determine if there is an ideal set of strategically-chosen viewing angles that can be used to most accurately determine the full BRDF with a minimum number of observations.

5. Effect of clouds on the TOA BRDF

Observations of clouds over snow have shown that the presence of clouds reduces the reflectance into near-nadir angles while enhancing reflectance into large nadir angles, especially into forward-scattering azimuths. This is particularly noticeable in MISR data (L. Di Girolamo 2005, personal communication), and was also observed at Dome C when thin fog formed between the surface and the top of the tower. Loeb (1997) suggests this enhancement of the forward scattering peak is due either to the cloud layer redirecting much of the incident light into the forward scattering direction, reducing the amount that can be reflected by the bright surface into near-nadir directions, or to shadowing of the surface by the clouds.

DISORT will be used to model the effect that a cloud layer placed over a snow surface has on the TOA BRDF. Cloud particles are generally smaller, and therefore should be more forward-scattering, than snow grains, casting some doubt on the first explanation given by Loeb. A possible alternative explanation is that the clouds over the ice sheets are optically smoother than the snow, i.e. the horizontal variations in the height of the top of the cloud layer are smaller, in units of optical depth, than the horizontal variations in the height of the snow surface. This idea will be tested by modeling the TOA BRDF of a cloud over an idealized, smooth snow surface and comparing that to the results when the measured BRDF of real snow surfaces are used as the lower boundary.

Several observations of the BRDF of thin fog layers over the snow were made at Dome C. The fog layer, often thinner than 30 m, caused a significant enhancement of the forward scattering peak, noticeable by eye, and clearly standing out in the data. DISORT will also be used to try to better understand these observations.

Additionally, these model results for various cloud optical depths can be examined to determine if there is one optical depth that can result in a TOA BRDF equal to the

observed monthly average.

6. Effect of clouds on radiation budgets

The effect of clouds over the Antarctic Plateau on the amount of solar energy absorbed at the surface or by the snow-atmosphere system (shortwave cloud radiative forcing, SWCRF) has not been adequately quantified.

ERBE, which has helped to quantify SWCRF over much of the planet, has failed to do so for the polar regions because of an inability to accurately identify clouds with their data set. Global values of TOA SWCRF measured by ERBE were published by Harrison et al. (1990), and they show positive values of SWCRF (indicating clouds cause increased absorption of sunlight by the snow-atmosphere system) over the Antarctic Plateau. However, Harrison et al. cautioned that the “results in the vicinity of the Arctic and Antarctic should be used with considerable caution” because of the problems in cloud identification. Similarly, Ramanathan et al. (1989) presented SWCRF measured by ERBE during April, showing positive values over the Arctic (there was very little sunlight reaching the Antarctic), a result that stood out dramatically on the cover of *Science*, reproduced in Figure 5. They cautioned that results over the Arctic are less certain than elsewhere and “even the sign of the effect may be uncertain.”

The problem of cloud identification using satellites is not just a matter of cloudy scenes being labeled clear. Yamanouchi and Charlock (1995) stated that, during the period they studied, most of the overcast reports by ERBE at South Pole occurred during clear skies. This problem suggests that the sign of the SWCRF reported by ERBE may well be incorrect if they are identifying mostly clear scenes as cloudy.

Sohn and Robertson (1993) compared ERBE-derived SWCRF with that computed using four other estimates and showed that all of the estimates except ERBE’s suggested

AMERICAN
ASSOCIATION FOR THE
ADVANCEMENT OF
SCIENCE

SCIENCE

6 JANUARY 1989
VOL. 243 ■ PAGES 1-140

\$3.50

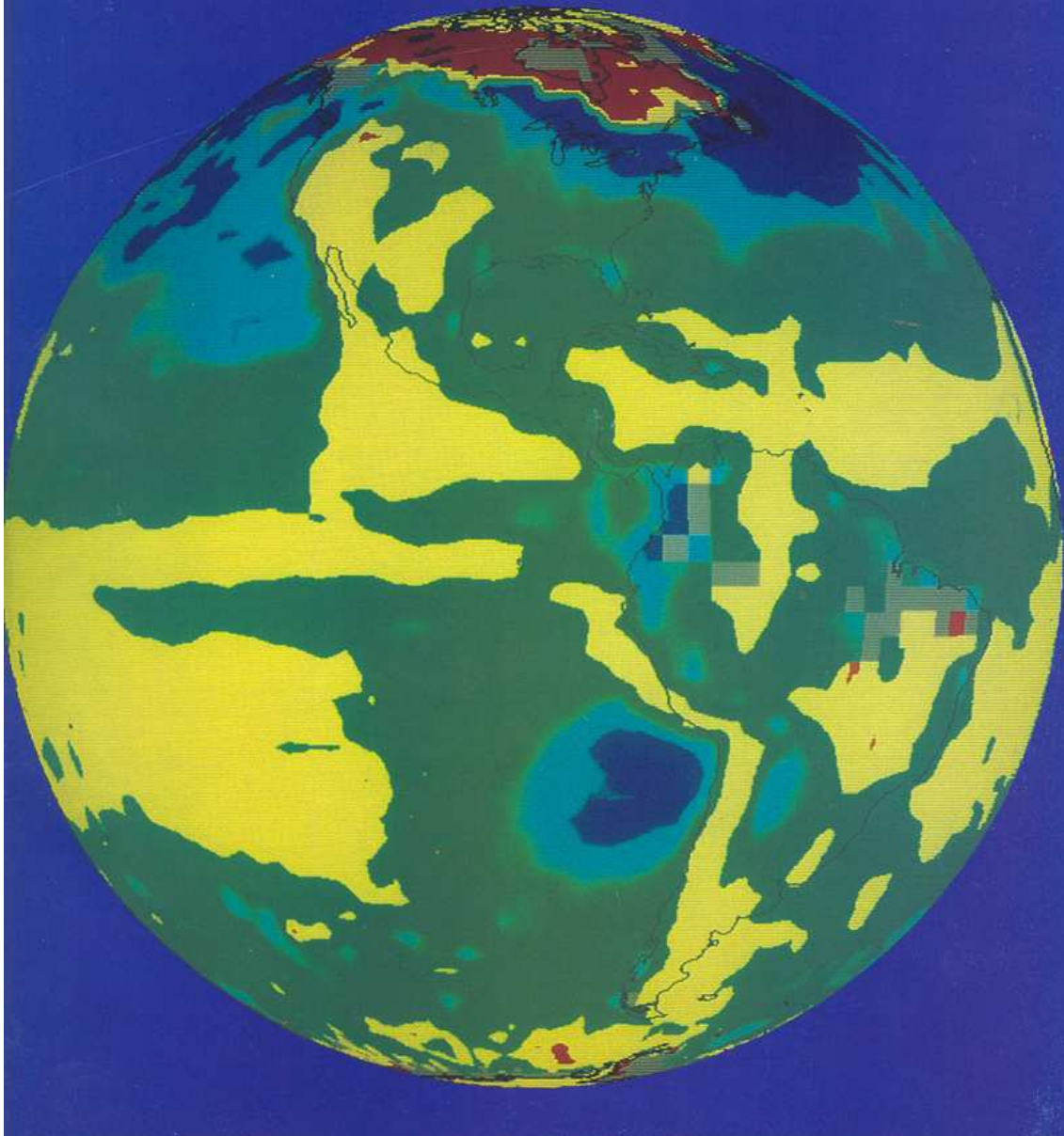


Figure 5. The cover of the 6 January 1989 issue of *Science* shows ERBE-derived TOA SWCRF (Ramanathan et al. 1989) for the Western Hemisphere in April. The positive values, indicated by the dark red and gray colors, stand out over northern North America.

that the TOA SWCRF in Antarctica was near zero.

Surface SWCRF estimates by ERBE suffer from the same problems of cloud identification. Pavolonis and Key (2003) estimated surface SWCRF on the Antarctic Plateau using two satellite-derived cloud data sets, the AVHRR Polar Pathfinder and the International Satellite Cloud Climatology Project. They found surface SWCRF values ranging from about -5 to -30 W m^{-2} , depending on location and month. The two data sets they used did not agree with each other, and likely have some problems identifying clouds despite being designed to work better in polar regions. Surface observations of surface SWCRF on the Antarctic Plateau are limited because of the few interior stations.

Using the ATRAD model with the observed surface BRDF as the lower boundary, the effect of clouds on the surface and TOA solar energy budgets will be calculated as functions of cloud optical depth. These modeling results will be combined with cloud optical depths estimated from the PAERI radiance measurements during summer at South Pole and Dome C to produce estimates of the surface and TOA SWCRF over the Antarctic Plateau. These results will then be compared to previously reported estimates from both satellite and surface measurements.

7. Atmospheric gases and solar radiation budget

Although the atmosphere is largely transparent to solar radiation, there are some regions of the solar spectrum in which absorption by carbon dioxide, ozone, and water vapor are significant. The ATRAD model, with observed surface BRDFs used as the lower boundary condition, will be used to investigate some of the effects of absorption of sunlight by these gases over the Antarctic Plateau.

This model will be used to investigate how these three gases affect both the surface and the TOA albedo of Antarctica. Unlike over most of the earth, in this region the

TOA albedo is observed to be lower than the surface albedo; this is largely due to atmospheric absorption [e.g. Warren (1982, Figure 12b) showed the spectrally-averaged surface albedo was around 82%, and the TOA albedo was around 72% for $\theta_o = 60^\circ$]. The role that each of the absorbing gases plays in this albedo reduction will be determined.

Observations by ERBE have shown that the TOA broadband albedo over snow decreases with solar zenith angle, while surface observations show the opposite relationship. The model will be used to see if atmospheric gases explain this difference and, if so, to identify which ones play the largest roles.

Most natural surfaces are significantly darker than snow. In most regions much of the sunlight that reaches the surface is absorbed, meaning the atmosphere is significantly affected only by incoming sunlight. However, over bright surfaces, like snow, the large amount of reflected sunlight gives the atmosphere a second shot at absorbing sunlight. This second chance is not equal to the first because the reflected light is traveling at different angles than the incoming light. Therefore, a bright surface can significantly enhance atmospheric absorption.

At least two features of the Antarctic atmosphere may be interesting to examine due to this enhanced absorption. The first is what effect the reflected light has on solar absorption by the ozone layer. How much is the temperature of this layer increased by absorption of reflected light, and how would it be affected if the albedo of the snow were to change? The second is to see if halving (representing ice-age conditions), doubling or quadrupling carbon dioxide levels has any significant effect on the solar radiation budget in Antarctica.

References

- Grenfell, T. C., S. G. Warren and P. C. Mullen, 1994: Reflection of solar radiation by the Antarctic snow surface at ultraviolet, visible, and near-infrared wavelengths. *J. Geophys. Res.*, **99**, 18 669–18 684.
- Harrison, E. F., P. Minnis, B. R. Barkstrom, V. Ramanathan, R. D. Cess and G. G. Gibson, 1990: Seasonal variation of cloud radiative forcing derived from the Earth Radiation Budget Experiment. *J. Geophys. Res.*, **95**, 18 687–18 703.
- Kou, L., D. Labrie and P. Chylek, 1993: Refractive indices of water and ice in the 0.65- to 2.5- μm spectral range. *Appl. Opt.*, **32**, 3531–3540.
- Loeb, N. G., 1997: In-flight calibration of NOAA AVHRR visible and near-IR bands over Greenland and Antarctica. *Int. J. Remote Sensing*, **18**, 477–490.
- Nicodemus, F. E., J. C. Richmond, J. J. Hsia, I. W. Ginsberg and T. Limperis, 1977: *Geometrical Considerations and Nomenclature for Reflectance*. NBS Monograph 160. National Bureau of Standards.
- Pavolonis, M. J. and J. R. Key, 2003: Antarctic cloud radiative forcing at the surface estimated from the AVHRR Polar Pathfinder and ISCCP D1 datasets, 1985–93. *J. Appl. Meteor.*, **42**, 827–840.
- Ramanathan, V., R. D. Cess, E. F. Harrison, P. Minnis, B. R. Barkstrom, E. Ahmad and D. Hartmann, 1989: Cloud-radiative forcing and climate: Results from the Earth Radiation Budget Experiment. *Science*, **243**, 57–63.
- Sohn, B. J. and F. R. Robertson, 1993: Intercomparison of observed cloud radiative forcing: A zonal and global perspective. *Bull. Amer. Meteor. Soc.*, **74**, 997–1006.

- Stamnes, K., S. Tsay, W. Wiscombe and K. Jayaweera, 1988: Numerically stable algorithm for discrete-ordinate-method radiative transfer in multiple scattering and emitting layered media. *Appl. Optics*, **27**, 2502–2509.
- Suttles, J. T., R. N. Green, P. Minnis, G. L. Smith, W. F. Staylor, B. A. Wielicki, I. J. Walker, D. F. Young, V. R. Taylor and L. L. Stowe, 1988: *Angular Radiation Models for Earth-Atmosphere System, Volume 1–Shortwave Radiation*. NASA Reference Publication 1184. National Aeronautics and Space Administration.
- Warren, S. G., 1982: Optical properties of snow. *Rev. Geophys. Space Phys.*, **20**, 67–89.
- Warren, S. G., 1984: Optical constants of ice from the ultraviolet to the microwave. *Appl. Opt.*, **23**, 1206–1225.
- Warren, S. G., R. E. Brandt and P. O. Hinton, 1998: Effect of surface roughness on bidirectional reflectance of Antarctic snow. *J. Geophys. Res.*, **103**, 25 789–25 807.
- Wiscombe, W. J. and S. G. Warren, 1980: A model for the spectral albedo of snow, I, Pure snow. *J. Atmos. Sci.*, **37**, 2712–2733.
- Wiscombe, W. J., R. M. Welch and W. D. Hall, 1984: The effects of very large drops on cloud absorption. Part 1: Parcel models. *J. Atmos. Sci.*, **41**, 1336–1355.
- Yamanouchi, T. and T. P. Charlock, 1995: Comparison of radiation budget at the TOA and surface in the Antarctic from ERBE and ground surface measurements. *J. Climate*, **8**, 3109–3120.